Power delay profile for 5G Network Utilizing Channel Simulator

Nishanthi Chilukuri
Computing Department
Bournemouth University
Bournemouth, United Kingdom
s5509588@bournemouth.ac.uk
ORCID:0000-0002-7299-9912

Santoshkumar Alagu
Computing Department
Bournemouth University
Bournemouth, United Kingdom
s5534784@bournemouth.ac.uk
ORCID:0000-0001-6557-6973

***Abstract*— Wireless communications are gaining massive demand for faster video streaming, virtual reality, and 5G-based IoT (Internet of Things) applications. Due to this network congestion increases hastily. The demand for user-specific services, machine learning, forcing the radio access network (RAN) to provide improvement in utilization of spectrum efficiency, minimizing power consumption, and improving data rate. For LTE/LTE-A network specifications provided by third-generation partnership project (3GPP), guarantees to provide qualitative of service (QoS). Release 15/16 utilizes two-dimensional (2D) active antenna array systems (AAS). This kind of AAS provides beam forming in both azimuth and elevation also termed as Full Dimensional MIMO (FD-MIMO). It enhances the radiation pattern of the antenna array element by adjusting the angular power spectra at the base station (BS), it also allows selecting the minimum number of antennas for effective beam forming toward specific user equipment's (UEs). Spectrum allocation challenge can be dealt with at mm wave band having FR2 (>6GHz) frequency band specified by International Telecommunication Union (ITU-R) in line with IMT-2020 specifications. The spectrum is free at mm Wave for communication of 5G. However, the main challenge is, it faces path loss and atmospheric loss electromagnetic energy absorbed by gases like oxygen. In this work, the 5G new RAN power spectrum and power delay profile at 10GHz carrier frequency with 20MHz to 100MHz channel bandwidth is observed for line of sight (LOS) and non-line of sight (NLOS) communication for guaranteed QoS. To demonstrate the path loss and power delay profile (PDP) in directional and Omni-directional antennas NYUSIM channel simulator is utilized.**

Keywords*— *FD-MIMO, LTE/LTE-A, New 5G RAN, NYUSIM, Power delay profile, power spectrum.

I. INTRODUCTION

Modern cellular communication systems like 4G LTE/LTE-A lack communication bandwidth due to the increasing demand for wireless communication across a wide variety of applications. To meet this rising demand, it is possible to use the unlicensed frequency spectrum, specifically the >6GHz band. Underutilized here, this spectrum is also known as the millimeter wave band. Fifth generation (5G) wireless technology is predicated on millimeter-wave (mmWave) communication. It is also uncommon to use large uniform antenna arrays for characterizing multiple mmWave bands and channels in a single set of measurements. Evaluating potential future air interfaces requires accurate channel models operating in the cellular frequency band [3]. Committees such as Mobile and wireless communications Enablers for the Twenty-twenty Information Society (METIS), Milli meter-Wave Evolution for Backhaul and Access (Mi-WEBA), WINNER II, COST 2100, ITU-R, and 3GPP have standardized current LTE/LTE-A channel models. The statistical spatial channel model created by researchers at New York University (NYU) and their contemporaries is referred to as NYUSIM [15].

5G wireless frameworks can utilize the mmWave frequency band to provide numerous benefits, including high data rates, maximum spectral efficiency, energy efficiency improvement, minimal signal-to-noise ratio (SNR), increased throughput, and so on. The mmWave region of the electromagnetic spectrum, also known as the Extremely High Frequency (EHF) range, covers frequencies between 30 GHz and 300 GHz. The range from 10 GHz to 30 GHz shares many similarities with EHF. That's why it's considered Ultra-High Frequency (UHF) as well. The transmission of large amounts of data is one of mmWave primary and significant applications [12]. In contrast to 4G, users of 5G networks will have access to significantly more spectrum allocations in previously unexplored mmWave frequency bands. To reduce infrastructure costs and increase aggregate capacity for many concurrent users operating in licensed and unlicensed bands, beam-forming antennas can be customized for each user. A compromised user's device or base station would cause high bit rates across large portions of the coverage area. While Release 15 of 3GPP's efforts resulted in the highly successful LTE-A, the work of standardizing 5G and exploring the possibilities of 5G continues to evolve as Release 16 and beyond [1]. By 2020, Release 16 of 5G will include support for high-capacity standalone (SA) connections, which will allow for maximum data transmission with minimal control overheads via 5G New Radio (NR) networks [4], and [5].

The mmWave frequency band is viewed as a favorable band to provide the services to vast number of users with unimaginable capacity [1] due to the large amount of channel band available. There are three distinct mmWave channels included each of which can be either directional, semi-omnidirectional, or sectorized [2]. Unfortunately, severe free space path loss and foliage loss negatively impact the accuracy of the channel modeling, preventing the system from going above and beyond the expectations of 5G users in terms of sub-terahertz technology includes imaging, wireless cognition, and precise positioning are taken to develop new design model and evaluation producer [3].

 doi:10.20944/preprints202212.0302.v1

Migrating user terminals (UTs) within the local coverage (10-15 m) [4] can show a consistent environmental profile despite their proximity to one another.

Furthermore, there should be a strong relationship between the channel impulse responses (CIRs) of these nearby positions. A spatially consistent channel model can generate correlated and time-variable channel coefficients [4], [7]. Power delay profiles (PDPs) and angular power spectra (APS) can be simulated in sequence from the UT path. For mmWave systems, human obstruction is a critical factor in radio signal strength, whereas it attracted little attention in the microwave (sub-6 GHz) frequency region. [18]. Directed antennas make it possible to minimize interference from people, but the distance at which this is possible is only a few millimeters at most. These are the most crucial terms to keep in mind when performing a link budget analysis [9] in the event of a vehicle investigation. As demonstrated by measurements and models [1], [18], [21], Outdoor-to-indoor (O2I) concerned with high propagation loss at mmWave frequencies due to concrete wall and infrared reflecting (IRR) glass [11]. Therefore, it is an important concept to consider when developing a new channel modeling for mmWave communication systems for use both indoor and outdoor [12].

The remaining sections of this paper are arranged as follows. The implications of the 3D channel space model for route loss and beam shaping of the ULA antenna array are discussed in Section II. Spatial continuity, human blockage, and O2I diffusion are taken into account when building the NYUSIM channel model. Section III presents the numerical results from the model validation. In Section IV, incorporated the output figures from NYUSIM v3.1 along with a menu for modifying the parameters to reduce interference from user input. The final paragraph, which includes some closing remarks, prepares the path for this field's future potential.

II. Related Work

The path loss determined by radio system Engineers at 0 dBi gain should have information of power received at specific distance of transmitter and receiver (T-R) of omnidirectional path loss models. This facilitates them to incorporate various channels with different kinds of antenna patterns. To date, numerous omnidirectional path loss models have been created. In which the path loss is determined as a function of various characteristics, such as distance in meter, frequency band; antenna steering, heights of transmitter and receiver. Many 3G and LTE/LTE-A [16] FD-MIMO radio systems use geometry-based stochastic 3GPP and WINNER II statistical spatial channel models (SSCMs). Furthermore, SSCMs provide weighted channel coefficients depending on propagation measurements in the effect of real-world. These measurements conducted between 1 GHz and 6 GHz for mmWave band and bandwidths ranging from 5 MHz to 100 MHz for RF signal in a variety of circumstances. At mmWave band, frequencies have substantially greater bandwidths and sharper angular resolution with time delay of order 20ns. The floating model is the result of omnidirectional path loss models provided by 3GPP and WINNER II. The method of SSCMs and minimum mean square (MMSE) best fit line concept is utilized to calculate minimum error for path loss with distances in log scale. That is in correspondence to the spectrum of measured distances. This model, which derives from best fit line model of MMSE utilizes a nearest spatial distance d0 across which spatial propagation is assumed. When fitting the MMSE best fit line, the close-in free space reference distance model is created by constraining the fit to an anchor point at the nearby spatial distance d0 (under the assumption that free space propagation is possible up to d0), where the slope of the best fit line and the standard deviation beyond d0 are referred to as the path loss exponent (PLE) and shadowing factor, respectively. In a similar way, but without the anchor point constraint, the floating intercept model which is also referred as moveable model is generated. Moveable model only offers the best fit to received path losses using MMSE concept on the other hand spatial model offers deep insights into propagation characteristics of channel[11],[19].

5G RAN deployed in Time Division Duplexing (TDD), mmWave bands, and Frequency division duplex (FDD). Active antenna array systems use a hybrid beam forming method to improve the efficiency of 5G technology. The selection and tracking of beams are defined by 3GPP reveal terminal flexibility. Today's traffic demands have led to a shortage of available bandwidth in the 3 to 6 GHz range. The remaining sub-3 GHz bands are critical to supporting 5G RAN implementations with 5G NR-only modes, supplemental uplink modes, aggregation of carriers, or dynamic spectrum sharing methods, but operators cannot use spectrum dedicated to 5G RAN. In addition to , the importance of high-performance passive antennas in next-generation wireless frameworks continues to increase [4]. Using all the available bandwidth above 300 GHz is one solution to the complications caused by this issue [3]. If mmWave and FD-MIMO are used together, they can significantly boost both wireless access and throughput for users in the field. Also, systems benefitted from enormously available spectrum bandwidth and base station form factor. MU- MIMO has proved its capability to improve network capacity by using a 2D active antenna array system and 8 x 8 radios TXR module in antenna (transmit and receive). In Massive MU-MIMO the number of antennas increases for licensed spectrum or unlicensed spectrum. Due to many antennas, spatial correlation, and channel weight vectors [2] increases. The antenna's RF front end integration allows for reasonable regulation of RF losses and passive inter modulation (PIM). At the same time, the increasing number of TXR arrays brings into sharper focus the massive MU-MIMO antenna's power consumption [4], [6]. FD-MIMO is best known as 2D active antenna array system (AAS). It not only produces beam forming in both azimuthal and elevation domains in 3D space but also adapts dynamically towards User Equipment [6], [9]. The spacing of each element is important in azimuth and elevation beam pattern performance. The azimuth beam is formed by considering each column as a separate element, while the elevation beam is formed by considering the vertically separated sub-arrays as the features. Azimuth beam forming typically uses several horizontally divided columns [10] to represent typical urban macro-cell and micro-cell environments, with urban macro cell (UMa), urban microcell (UMi), and a-high rise (UMa-H) being the most common. Under LoS, NLoS,

Preprints (www.preprints.org) | NOT PEER-REVIEWED | Posted: 16 December 2022 doi:10.20944/preprints202212.0302.v1

and outdoor-to-indoor propagation scenarios [2], the 3GPP 3D channel model specifies three propagation conditions for user equipment (UE) (O-to-I). Each UE [13] uses its own unique combination of path loss, average propagation speed, and macroscopic and microscopic fading to establish its own unique distance at which communication is lost. Probability of entering a LoS state is calculated independently for indoor and outdoor UEs based on UE height and breakpoint distance. FD-MIMO beam forming pattern at transmitter side is given by (1)

$$A_{E(\emptyset_{tA}\theta_{tE})} = G_{e,max} - \min\{A_{E,H}(\emptyset_{tA}) + A_{E,V}(\theta_{tE}), A_m\} \quad (1)$$

FD-MIMO beam forming pattern at the receiver side is given by (2)

$$A_{E(\emptyset_{tA}\theta_{tE})} = G_{e,max} - \min\{A_{E,H}(\emptyset_{rA}) + A_{E,V}(\theta_{rE}), A_m\} \quad (2)$$

Where radiation pattern at transmitter and receiver is represented by [12] $A_E(\emptyset_{tA},\theta_{tE})$ and $A_E(\emptyset_{rA},\theta_{rE})$, also $\emptyset_{tA}$, θ_{tE} are azimuthal and elevation angles at the transmitter. $A_{E,H}(\emptyset_{tA})$ represents the horizontal beam forming and $A_{E,V}(\theta_{tE})$ vertical beam forming representation at the transmitter. A_m antenna attenuation assumed the same at both transmitter radiation pattern and receiver radiation pattern. $G_{e,max}$ directional gain considered as 10dBi at both transmitter and receiver $\emptyset_{rA}$, θ_{rE} are azimuthal and elevation angles at the receiver. $A_{E,H}(\emptyset_{rA})$ is the horizontal beam forming and $A_{E,V}(\theta_{rE})$ vertical beam forming representation at receiver[7]. Path loss model supported by NYUSIM for 2D active antenna array system is given by [12], [15].

$$PL^c(f,d)|dB| = FSPL(f,1m)|dB| + 10n\log_{10}(d) + AT|dB| + \chi_\sigma^{CI} \quad (3)$$

Where f is the carrier frequency, d is the Tx-Rx separation distance (considered to be $d \geq 1m$), n is the path loss exponent (PLE), c is the velocity of light, AT be the atmosphere attenuation coefficient, χ_σ^{CI} is a zero-mean Gaussian random variable with standard deviation in dB, and $FSPL\ (f,1m)$ represents path loss (dB) in the free space at distance of 1m between Tx and Rx [8]. Hence, it is mathematically defined as

$$FSPL(f,1\ m)|dB| = 20log_{10}\left(\frac{4\pi fX109}{c}\right) = 32.4|dB| + 20log_{10}(f) \quad (4)$$

$$AT|dB| = \alpha|dB/m| \times d[m] \quad (5)$$

3D space propagation model and 8x8 FD-MIMO arrangement in Uniform linear array model [1],[15],[16] is shown in below Fig1 and 2. In Fig 1 Type I codebook selects strongest beam out of all the beam forming generated from antenna array in type II codebook weights of beams selected and the optimized channel matrix is calculated according to depending on Maximal ratio combining technique (MRC). In type II codebook, aggregate of weighted average of all beams is assigned per sub band taken. Fig 2 represents 3D channel space model for FD-MIMO beam forming in both azimuth and elevation angles.

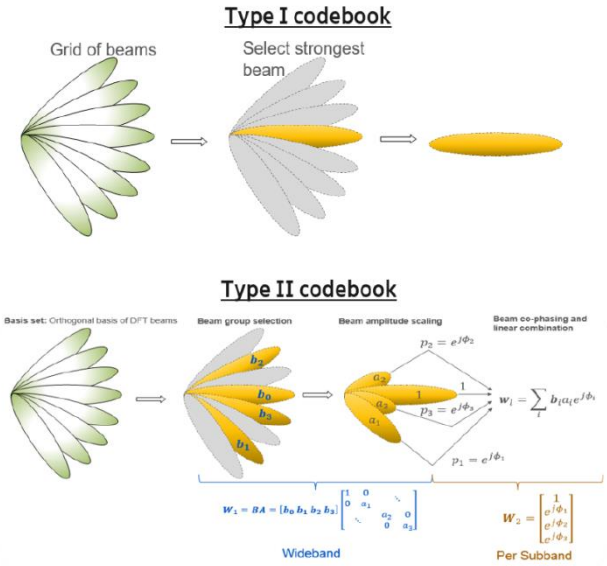

Fig.1 3D -beam forming antenna array pattern

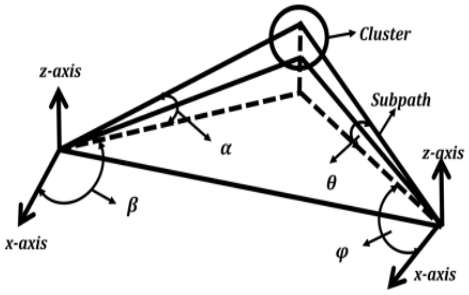

Fig.2 Channel space model

This paper uses a NYUSIM channel simulator to analyze the performance of a 5G network in terms of power spectrum and power delay profile while operating in the 10 GHz frequency range and considering LOS, NLOS, UMi, and UMa scenarios with large antenna arrays. Clusters strategy in the 3GPP model is entirely dependent on a joint delay-angle probability density function. This channel simulator is capable for analyzing in both statistical and deterministic channel models. For studying adaptive beam forming i.e., FD-MIMO processing requires spatial consistency for use in mobile scenarios. These channel models statically rely on both large-scale parameters and small scale parameters. The focused large scale parameters are delay spread, directive beam forms, time clusters (TC), and angular spread. For each multipath component(MPC) small-scale parameters are angles of (AoA) and angles of departure (AoD), beams arrival time difference and power from measurements[13], [20]. On the other hand deterministic channel models depend on ray-trace methodology and area [12], [20].The average multipath delay is calculated by combining the AoD and arrival AoA, which is known as cluster group formation [3], [21]. Likewise, the multipath behavior in an omnidirectional channel is described using the notions of time cluster (TC) and spatial lobe (SL), respectively. The travelling distance difference is estimated to identify the TCs these are categories under shortest propagation. The primary directions of energy arrival over several hundred ns are indicated by SLs. TC arrive close in time from different SL due to multipath components includes angular directions,

Preprints (www.preprints.org) | NOT PEER-REVIEWED | Posted: 16 December 2022 doi:10.20944/preprints202212.0302.v1

decoupling temporal, and spatial statistics. Thereby, both exists some difference in time delay. This difference is estimated in [15] from propagation delay measurements (nanoseconds) which takes energy arriving or departing by high gain rotatable directional antennas in a specific direction. In order to extract TC and SL statistics from any measurement or ray-tracing data sets [15],[8],[21], one must make sure that the propagation time between the user and the obstructions is as short as possible.

III. Proposed Work

For power profile analysis, a channel simulator was employed. In this work findings are based on the propagation of 28-73 GHz mmWave channels in a variety of real-world settings, including rural macrocell (RMa), urban macrocell (UMa), and urban microcell (UMi). In both the frequency and time domains, it allows for precise channel responses. Moreover, the measured signal values are valid for RF bandwidths spanning 0 to 800 MHz and carrier frequencies spanning 500 MHz to 100 GHz. NYUSIM is a channel simulator functioning in MATLAB scripts that works on any operating system thanks to its cross-platform GUI [17]. The programmed output response plots produced by the drop-based model are similar to the older versions of NYUSIM, as shown in [13]. The UT and BS locations are maintained together with the spatial consistency mode and geographically connected with SF. Its LOS/NLOS probability result indicates that there is a uniform propagation condition at all points in the local area. In order to demonstrate the power variation and latency drifts of MPCs, successive omnidirectional and directional PDPs are provided in the direction of intense MPC to the omnidirectional PDP. The 3D angular power spectrum for AOA and AOD is being captured at an angle that changes over time. After testing the beam steering mechanism, examining the dynamic channel state, and assessing the effectiveness of the MIMO system, results of the channel along the path are recorded for the values that vary with time and positional spaced values [18].

It can be observed in Fig. 3, the GUI divides the nearly thirty channel parameters into two distinct groups based on channel parameters and antenna properties. There are sixteen primary input parameters related to the channel through which the signal will be transmitted. Similarly, 12 spatial consistency parameters and 5 human blockage input parameters are included in the source and destination of radiation patterns. Tables I, II, and III indicates the additional input parameters utilized. The spatial consistency checks the user's position in a linear and hexagonal fashion. There's a pre-set value for human interference which can be adjusted according to specific requirement under human blockage parameters.

TABLE I. Antenna Parameters

Parameters	Values
Antenna-type	FD-MIMO
Beam forming	3D
Number of transmitters along x, W_t	8
Number of receivers along x, W_r	8
Transmitting antenna array	ULA
Receiving antenna array	ULA
Number of receive antenna elements Nr	8
Transmit antenna spacing λ_t	0.5
Receive antenna spacing λ_r	0.5
Transmit antenna azimuthal HPBW $Ø_{tA}$	65°
Transmit antenna elevation HPBW θ_{tE}	15°
Receive antenna azimuthal HPBW $Ø_{rA}$	65°
Transmit antenna elevation HPBW θ_{rE}	15°

TABLE II. Channel Parameters Line of Sight

Parameters	Values
Scenario	UMi
Environment	LoS
Frequency	10GHz
RF Bandwidth	100MHz
Polarization	Co-Pol
Transmit power P_t(dBm)	43.01
Base station Height	50m

TABLE III. Channel Parameters Non-Line of Sight

Parameters	Values
Scenario	UMi
Environment	Non-LoS
Frequency	10GHz
RF Bandwidth	100MHz
Polarization	Co-Pol
Transmit power P_t(dBm)	43.01
Base station Height	50m

The NYUSIM channel modeling procedure can be summarized as follows. For UMi scenario with 10GHz carrier frequency, then antenna parameters selection, and specifying the user's terminal mobility trajectory. The required space and time lobe parameters will be obtained for the entire model, respectively. For creating cluster in time after calculating sub paths that belong to corresponding cluster, the initial delay, power, and phase of the sub pathways are first formed. The methods used to generate the spatial lobe parameters match the time cluster. The model will allocate sub pathways to various spatial lobes after determining the number of spatial lobes, and it will compute the sub path angles based on the spatial lobe angles. Later, the transceiver's geometric relationships will determine how the user's movement affects the delay, power, angle, and phase. The birth-death mechanism of clusters is responsible for the transition between segments. The aforementioned modeling stages will result in channel parameters, which NYUSIM will produce based on the input parameters. The geometric relationship between various snapshots is used to update the angle parameters of a segment. The distribution of parameters will change at the start of each segment [3].

Figure 3 depicts the NYUSIM parameters selection window, which uses two basic files to define the input parameters, "BasicParameters.txt" and "BasicParameters.mat." Each of four unique columns in this file corresponds to a critical variable for one of the N omnidirectional PDPs from the N continuous simulation

Preprints (www.preprints.org) | NOT PEER-REVIEWED | Posted: 16 December 2022 doi:10.20944/preprints202212.0302.v1

runs. There are several components to it, including power, obtained, attenuation, and in all directions, omnidirectional path loss, and omnidirectional root-mean-square (RMS) delay spread. The "DirPDPInfo.txt" and "DirPDPInfo.mat" files are also included, and each of them has ten columns that indicate an essential value in directional PDPs from a number of outputs executed continuously. These parameters include latency, power obtained from receiver, phase, azimuth and elevation AODs and AOAs of each resolvable MPC (i.e., antenna pointing angle), directional attenuation, and delay spread. As illustrated in Fig. 10, each "AODLobePowerSpectrumn Lobex" file is linked to a 3D AOD power spectrum output image and includes five parameters: pathDelay (ns), pathPower (mWatts), pathPhase (rad), AOD (degree), and ZOD (degree) in each column of each resolvable MPC in an AOD spatial lobe. The spectrum radiation for LOS and NLOS is similarly shown in Figs. 9 and 11, respectively. It is created using the "AOALobePowerSpectrumn Lobex" supporting file, where each.txt and.mat file is used to adjust parameter values in a UMi scenario. Each "OmniPDPn" file contains two columns: propagation time delay in 10^{-9}sec and power at the receiver in dBm connected to an omnidirectional PDP output figure [17].

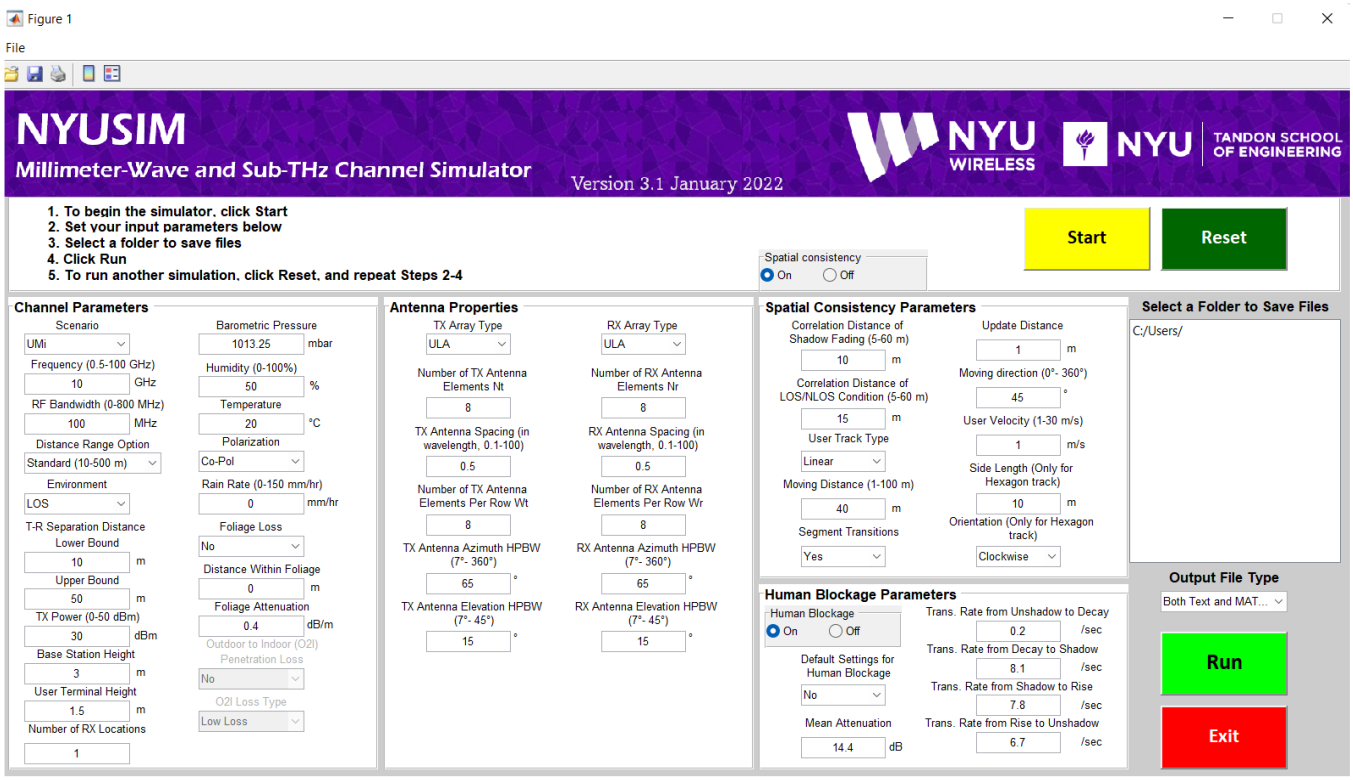

Fig. 3 NYUSIM parameter selection window

IV. Simulation Results

The simulation results are generated for various features such as spatial consistency, human blockage, and O2I penetration. These are constantly considered as the CIRs that vary over time. It was shown in Fig. 3 that the NYUSIM 3.1 version GUI is used to simulate the power spectrum and power delay profile caused by interference of human events. Typically, it would switch between two modes—the drop-based mode and spatial consistency mode—to ensure the optimal performance. The model uses buttons to switch between the modes, and one of them, labelled as "spatial consistency," in “ON” means activates a procedure that creates correlated CIRs in sequence with the UT trajectories. The switch set to "OFF" position automatically executes the drop-based model, which is the earlier versions of NYUSIM and produces separate CIRs for various distances. It is to be noted that the human blockage module is compatible with both drop-based and spatial consistency mode.

A. Simulation of UMi-LOS

Figures 4 to 10 are generated using UMi-LoS 8X8 FD-MIMO with ULA pattern, with antenna azimuthal and elevation HPBWs, at the TX and RX adjusted to 65^0 and 15^0, respectively. The 3D SCM radiation pattern for UE is determined from the antenna HPBWs used in the 10 GHz measurements (1), (2), (3), (4), and (5). The simulated AoA power spectrum, AoD power spectrum Omnidirectional PDP, Directional PDP, and small-scale power delay profile (PDP) measured with the values presented in Table I, II and Table III. The FD-MIMO antenna is used in conjunction with a spatial filter, based on the user's preferences, chooses the appropriate multipath components among projected beam forms. Due to this combination of FD-MIMO with spatial filter antenna configuration omnidirectional antennas always show greater path loss and partial reflection in comparison to directional antennas. Furthermore, the Receiver NLOS situation is the same as in LOS, but the beam detection process is slightly more complicated in NLOS [7],[9].

Preprints (www.preprints.org) | NOT PEER-REVIEWED | Posted: 16 December 2022 doi:10.20944/preprints202212.0302.v1

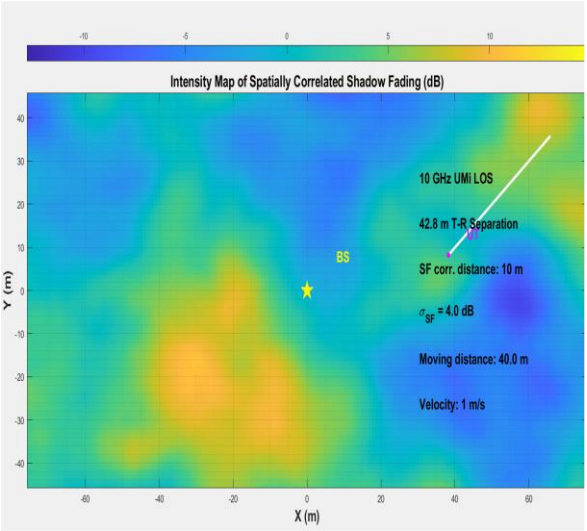

Fig. 4 Intensity map of spatial correlation with respect to FD-MIMO at mmWave

Fig. 4 depicts a 50 by 50 meter spatially correlated intensity map of SF with FD-MIMO. When operating in an UMi LOS configuration, the SF correlation distance is programmed to be 10 meter. As shown in Fig. 4, the User Terminal (UT) travelled 40 meters in a clockwise direction along a partial hexagon track. The SF has a smooth gradient between -10 dB and 10 dB. In contrast to the drop-based model, which always employs independent values for close locations, similar SF values are observed at closely spaced locations.

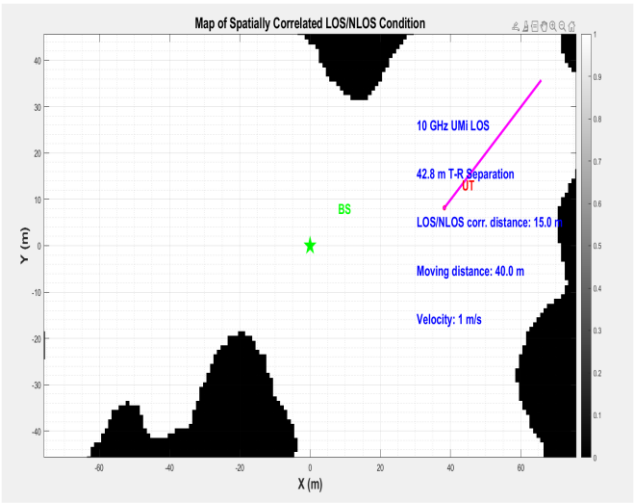

Fig. 5 Spatial correlation with respect to FD-MIMO at mmWave for LOS/NLOS

In Fig 5 spatial correlation with respect to FD-MIMO at mm wave band at a velocity of 1m/s is illustrated.

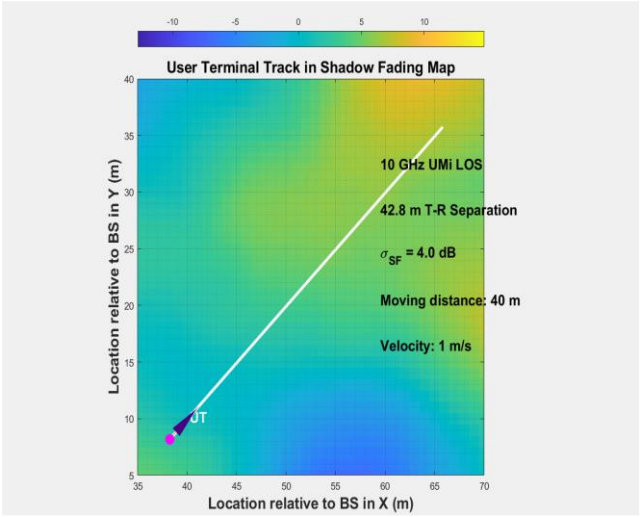

Fig. 6 Propagation map for shadow fading relative to BS

User terminal tracking with respect to base station at mmWave frequency band (carrier frequency of 10GHz) in shadow fading is depicted in Fig 6. Since, mobility of user is continuously changing, it is required to detect UT with respect to BS using beam forming technique to provide services to users even in the presence of fading.

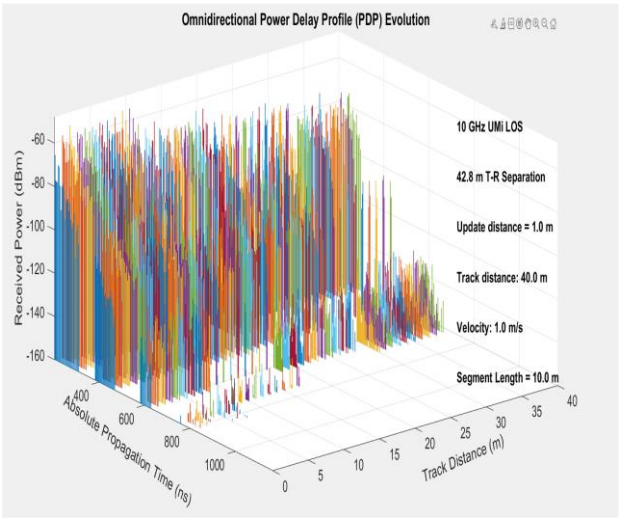

Fig. 7 Omni Directional Power Delay Profile at 10GHz carrier frequency

Omni directional and direction scattered power profile plot and power delay profile at mmWave band with moving distance of 10m are generated as shown in Fig 7, 8, 9 and 10 respectively. Fig 7 and 8 gives information of power delay profile at 10GHz carrier frequency with T-R separation of 42.8 m for LOS communication in 3D space with velocity of 1.0 m/s.

Preprints (www.preprints.org) | NOT PEER-REVIEWED | Posted: 16 December 2022 doi:10.20944/preprints202212.0302.v1

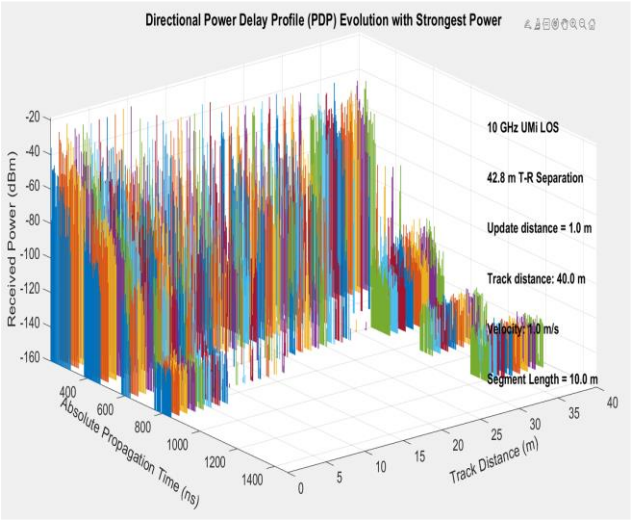

Fig. 8 Directional Power Delay Profile at 10GHz carrier frequency

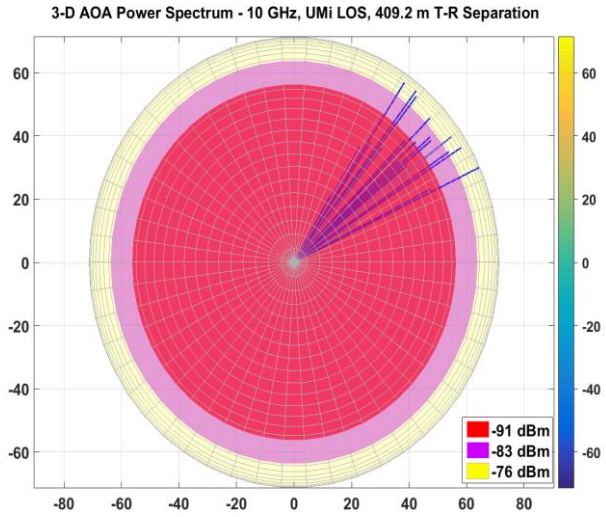

Fig.9 3D Angle of Arrival(AoA) Power spectrum of UMi-LoS.

Power delay profile of omnidirectional antenna array in ULA produces more loss of power introducing more fading, whereas directional antenna array uses steered beam forming technique, hence the later performs better with respect to usage of power. The radiation pattern of FD-MIMO in ULA for UMi LOS communication for both Angle of Arrival (AoA) and Angle of Departure (AoD) is shown in Fig 9 and 10.

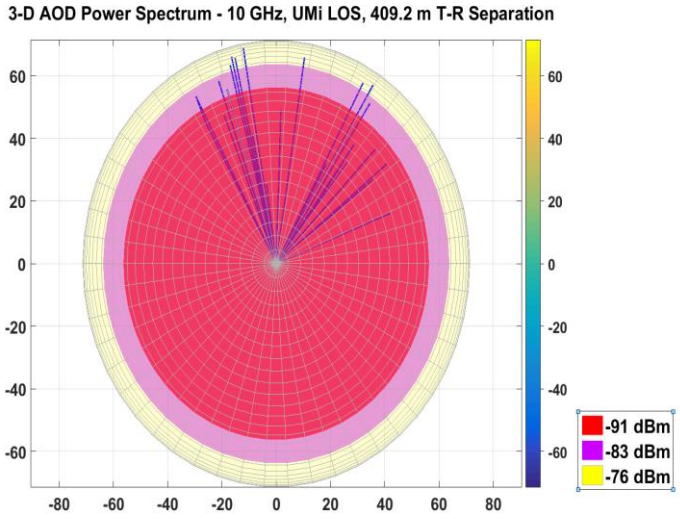

Fig. 10 3D Angle of Arrival(AoD) Power spectrum of UMi-LoS

B. Simulation of UMi-NLOS

The antenna azimuthal and elevation HPBWs at the TX and the RX were tuned to 65^0 and 15^0, respectively, to create the UMi-NLoS 8X8 FD-MIMO with ULA pattern illustrated in Fig. 11 to 17. It corresponds to the antenna HPBWs utilized in the 10 GHz tests. Equations (1) and (2) are used to calculate the 3D SCM radiation pattern for the UE, and equations (3), (4), and (5) are used to calculate the route loss for the model under study (5). The computed directional power delay profile, small-scale power delay profile, and omnidirectional power delay profile are shown in Tables I and III (PDP).

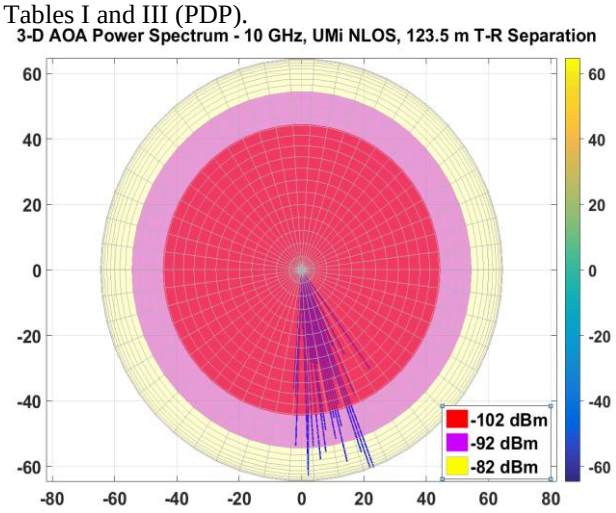

Fig. 11 3D Angle of Arrival(AoA) Power spectrum of UMi-NLoS

The radiation pattern of FD-MIMO in ULA for UMi NLOS communication for both Angle of Arrival (AoA) and Angle of Departure (AoD) is shown in Fig 11 and 12.

Preprints (www.preprints.org) | NOT PEER-REVIEWED | Posted: 16 December 2022 doi:10.20944/preprints202212.0302.v1

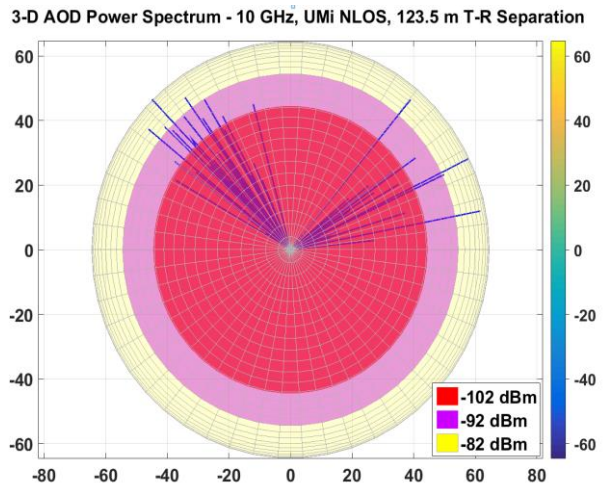

Fig. 12 3D Angle of Arrival(AoD) Power spectrum of UMi-NLoS

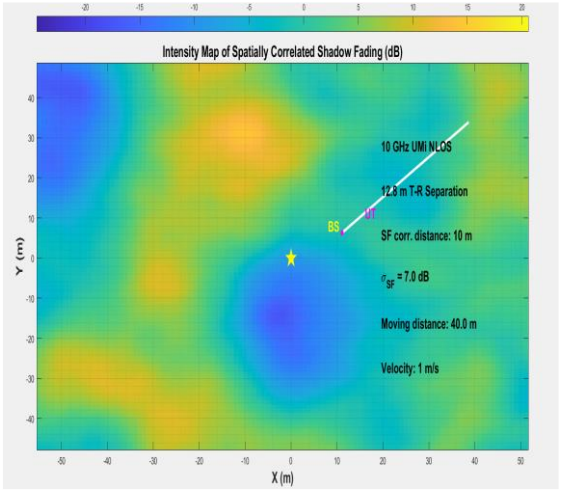

Fig. 13 Intensity map of spatial correlated shadow fading for UMi-NLoS

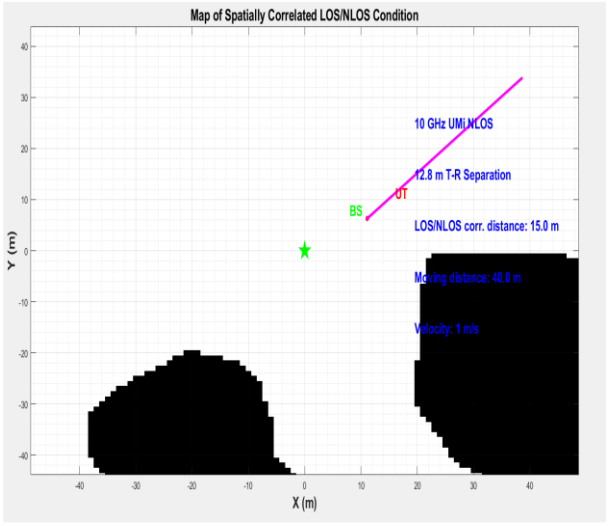

Fig. 14 Spatial correlation map of UMi-NLoS

Fig. 14 reveals spatial correlation with respect to FD-MIMO at mm wave band at a velocity of 1m/s for UMi NLOS. T-R separation is less in comparison to UMi-LOS.

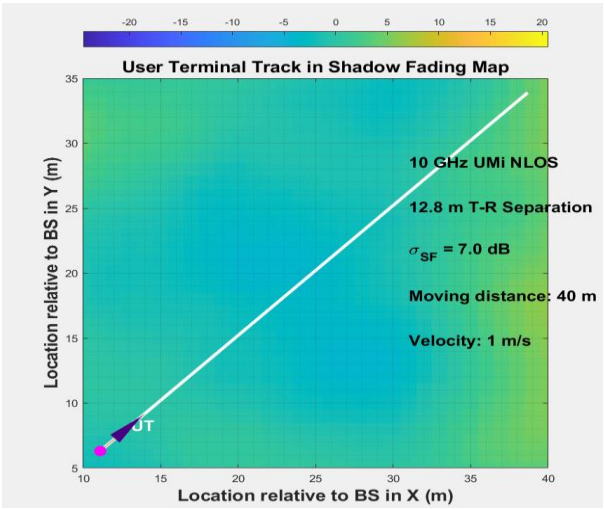

Fig. 15 User Terminal Track shadow fading for UMi-NLoS

As can be seen in Fig. 15, a partial hexagon tracking scenario ranging from 10 meters to 40 meters produces a clockwise-circling SF spatial correlation map over 50 by 50 meters. It can be noticed about SF for users close together and remaining further apart, both calculated from drop-based model, exhibit a continuous range from -10 dB to 10 dB. Similar to the UT trajectory, time-varying large and small-scale parameters such as LOS, NLOS, angle, delay, and power are evaluated, [19], [20] to ensure spatial consistency is maintained across all realistic channels. To obtain the readings, several channel segments are established, with a constant distance of 10 to 15 meters. Maintaining a high rate of spatial consistency allows increasing the likelihood that a spatial correction will occur. The channel coefficients of adjacent channels are likewise updated every 1 meter along a travelled path, so the spatial distance between them is periodically updated to reflect the actual distance travelled. Mobility of User is continuously changes so it is required to detect UT with respect to BS using beam forming technique to provide services to users even in the presence of fading in NLOS situation as of LOS, however it is little complex in NLOS the detection process of beam.

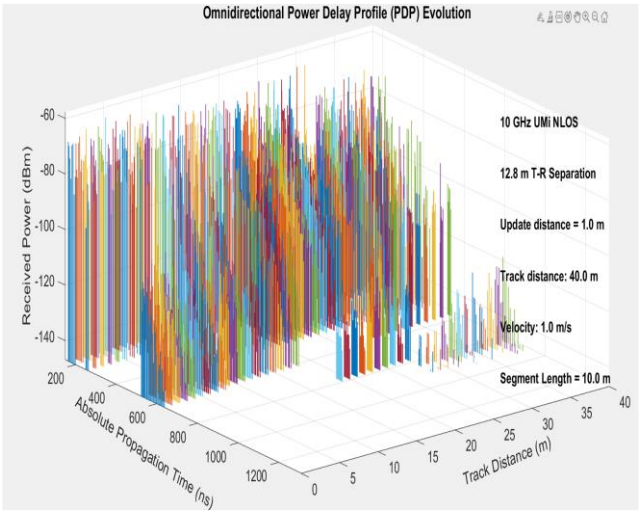

Fig. 16 Omni Directional Power Delay Profile for UMi-NLoS

Preprints (www.preprints.org) | NOT PEER-REVIEWED | Posted: 16 December 2022 doi:10.20944/preprints202212.0302.v1

Omni directional and direction scattered power profile plot and power delay profile at mmWave band with moving distance 10m are generated as shown in Fig 11,12,16, and 17 respectively for UMi-NLOS..Fig 16 and 17 gives information of power delay profile at 10GHz carrier frequency with T-R separation of 12.8 m for NLOS communication in 3D space. Power delay profile of omnidirectional antenna array in ULA produces more loss of power introducing more fading whereas directional antenna array uses steered beam forming technique, so it performs better with respect to usage of power.

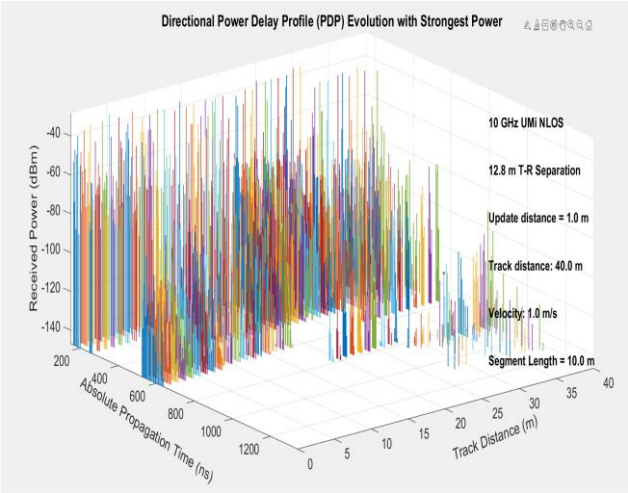

Fig. 17 Directional Power Delay Profile for UMi-NLoS

V. Conclusion

The NYUSIM release is a re-creation of the directional and omnidirectional PDPs or CIRs and channel statistics for a variety of carrier frequencies in both LOS and NLOS communications. Operating via its intuitive graphical user interface (GUI), it considers RF bandwidths, antenna beam widths, testing scenario, and weather conditions. Power spectra and power delay profiles of various configurations, including omnidirectional, directional, and small-scale path loss at mmWave frequencies, are analyzed by NYUSIM for the 3GPP model's radio network, which operates at sub-6GHz frequencies. An experimental investigation is carried out for the hybrid beam forming antenna technique for an FD-MIMO scenario to evaluate realistic mmWave frameworks where multiple antenna elements may be packed into a reasonable base station form-factor. The per-user spectral efficiency calculated by NYUSIM for a single-cell, three-user MIMO system is approximately 1.5 times higher than that produced by 3GPP other channel simulators when operating carrier frequency is taken into account. NYUSIM produces results that are in exquisite agreement with the observed data. Application examples for channel condition study are used to compare the 3GPP and NYUSIM models for analyzing the performance of an FD-MIMO channel. NYUSIM is useful for developing and deploying 5G communication systems.

References

[1] Shu Sun , George R. MacCartney; Theodore S. Rappaport,“ A Novel Millimeter-Wave Channel Simulator and Applications for 5G Wireless Communicationsm”, Paris, France,IEEE, IEEE International Conference on Communications (ICC), 21-25 May 2017.

[2] Rifat Hasan, Md Munjure Mowla, Nabila Hoquel, “Performance Estimation of Massive MIMO Dropbased Propagation Channel Model for mmWave Communication”, IEEE Region 10 Symposium (TENSYMP),Dhaka, Bangladesh, IEEE, pp.461–464, 5-7 June 2020, https://ieeexplore.ieee.org/document/9230462.

[3] Yaping He, Yang Zhang, Jin Zhang, Lihua Pang, Yijian Chen, and Guangliang Ren “Investigation and Comparison of QuaDRiGa, NYUSIM and MG5G Channel Models for 5G Wireless Communications” IEEE 92nd Vehicular Technology Conference (VTC2020-Fall), IEEE, Victoria, BC, Canada, 2020 https://ieeexplore.ieee.org/document/9348775.

[4] 5G Americas White Paper: “Advanced Antenna Systems for 5G” – 2019 , https://www.elsevier.com/books/advanced-antenna-systems-for-5g-network-deployments/asplund/978-0-12-820046-9.

[5] TR 21.915 "3rd Generation Partnership Project; Technical Specification Group Services and System Aspects; Release 15 Description; Summary of Rel-15 Work Items (Release 15)", 2019, 3GPP.

[6] Shu Sun and T. S. Rappaport, Timothy A.Thomas, Amitava Ghosh “Preliminary 3D mm wave indoor office channel model,” 2015 International Conference on Computing, Networking and Communications, (ICNC) 2015.

[7] Sekander S, Tabassum H, & Hossain E, “Multi-tier drone architecture for 5G/B5G cellular networks: Challenges, trends, and prospects.” IEEE Communications Magazine, 56(3), 96-103,2018.

[8] Mezzavilla, M., Zhang, M., Polese, M., Ford, R., Dutta, S., Rangan, S., & Zorzi, M. (2018). “End-to-end simulation of 5g mm-wave networks”. IEEE Communications Surveys & Tutorials.

[9] Emil Björnson, Erik G. Larsson, and Thomas L. Marzetta “Massive MIMO: Ten Myths and One Critical Question”, IEEE Commun. Magazine, vol. 54, no. 2, pp. 114 - 123, 2016.

[10] G. R. MacCartney et al., "Omnidirectional path loss models in new york city at 28 GHz and 73 GHz," in 2014 IEEE 25th Annual International Symposium on Personal, Indoor, and Mobile Radio Communication (PIMRC), Sep. 2014, pp. 227–231.

[11] T. S. Rappaport, S. Sun, and M. Shafi, "5G channel model with improved accuracy and efficiency in mm-wave bands," IEEE 5G Tech Focus, vol. 1, no. 1, Mar. 2017.

[12] 3GPP, "Study on channel model for frequency spectrum above 6 GHz," 3rd Generation Partnership Project (3GPP), TR 38.900 V14.2.0, Dec. 2016.

[13] Jaeckel, S., Raschkowski, L., Börner, K., & Thiele, L.. “QuaDRiGa: A 3-D multi-cell channel model with time evolution for enabling virtual field trials”. IEEE Transactions on Antennas and Propagation, 62(6), 3242-3256,2014.

[14] T. S. Rappaport, S. Sun, and M. Shafi, "Investigation and Comparison of 3GPP and NYUSIM Channel Models for 5G Wireless Communications", IEEE 86th Vehicular Technology Conference(VTC-2017), 2017.

[15] Reshma Ann Mathew and Ria Maria George "Measurements and Characterization of 5G Wireless Channel for mmWave Massive MIMO System with Circular Rayline Array Pattern" International Journal of Applied Engineering Research ISSN 0973-4562 Volume 13, Number 4 (2018) Spl.

[16] Shah Zeb , Aamir Mahmood, Syed Ali Hassan, Mikael Gidlund., “Analysis of Beyond 5G Integrated Communication and Ranging Services under Indoor 3D mmWave Stochastic Channels-2”, *IEEE* Transactions on Industrial Informatics, Volume: 18, Issue: 10,January 2022.

[17] Shu Sun , George R. MacCartney; Theodore S. Rappaport,“ A Novel Millimeter-Wave Channel Simulator and Applications for 5G Wireless Communicationsm”, Paris, France,IEEE, IEEE International Conference on Communications (ICC), 21-25 May 2017.

[18] Ju, S., O. Kanhere, Y. Xing, and T. S. Rappaport, "A millimeter-wave channel simulator NYUSIM with spatial consistency and human blockage" ,2019 IEEE Global Communications Conference (GLOBECOM), 1-6, Hawaii, USA, Dec. 2019.

[19] “Quantifying the Benefits of 64T64R Massive MIMO with Beamforming and Multi-User MIMO Capabilities," Signals Ahead, Part I. Vol. 14, No. 9, Nov. 29, 2018.

 doi:10.20944/preprints202212.0302.v1

[20] ——, “Millimeter-wave extended NYUSIM channel model for spatial consistency,” 2018 IEEE Global Communications Conference (GLOBECOM), pp. 1–6, Dec. 2018.

[21] M. K. Samimi and T. S. Rappaport, “3-D millimeter-wave statistical channel model for 5G wireless system design,” IEEE Transactions on Microwave Theory and Techniques, vol. 64, no. 7, pp. 2207–2225, Jul. 2016.